NRC research update

[1]Mengistu Wolde: IWC– W-band and X Dual-Frequency

[1]Cuong Nguyen: IWC – W-band and X-band Polarimetric

[1]Konstantin Baibakov: IWC - Elastic Lidar

[3]Philip Gabriel: IWC - G-band radiometer

&

[2]Alexei Korolev

1- National Research Council Canada

2- Environment and Climate Change Canada

3- General Analytic LLC

HAIC-HIWC Science Team Meeting, 16-19 May 2016

National Research Council Canada Conseil national de recherches Canada

Environment Canada Environnement Canada

Canada

W/X-band Dual – Frequency Analysis

NAWX - IWC vs. Z_e

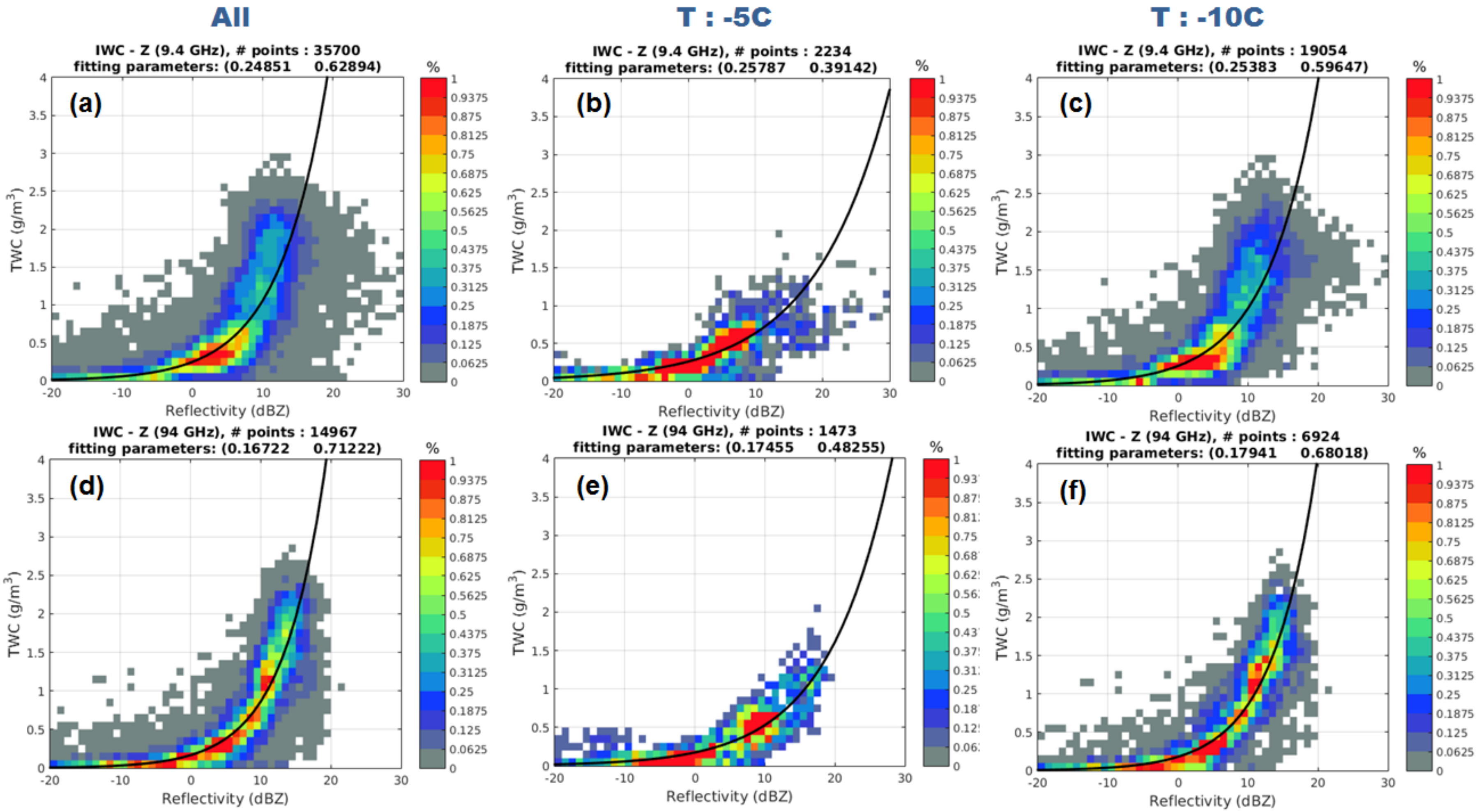

Environment Canada Environnement Canada

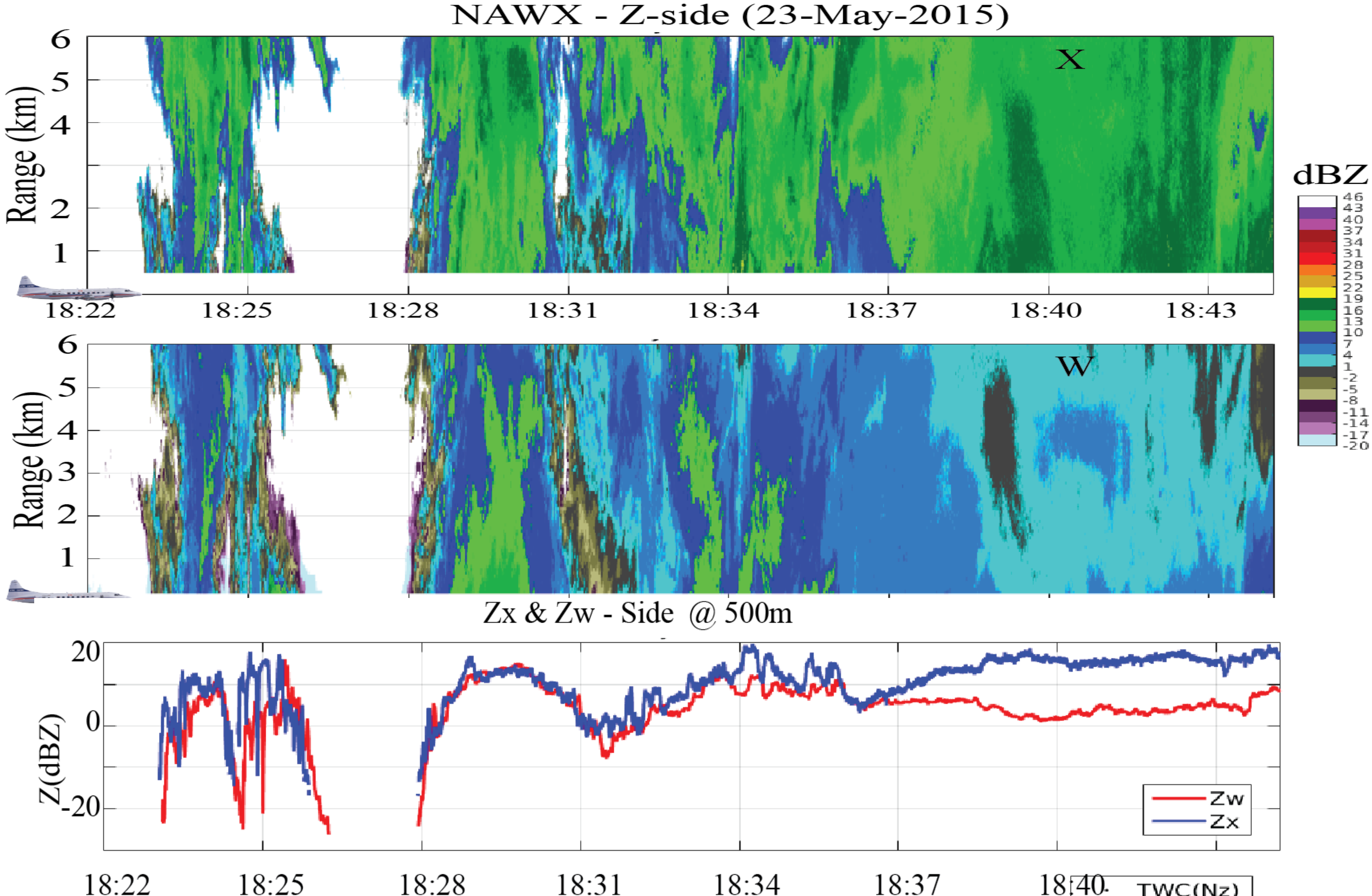
NAWX - Z-side (23-May-2015)
X
W
Range (km)
dBZ
Zx & Zw - Side @ 500m
Z(dBZ)
Zw
Zx
18:22
18:25
18:28
18:31
18:34
18:37
18:40
18:43
TWC(Nz)

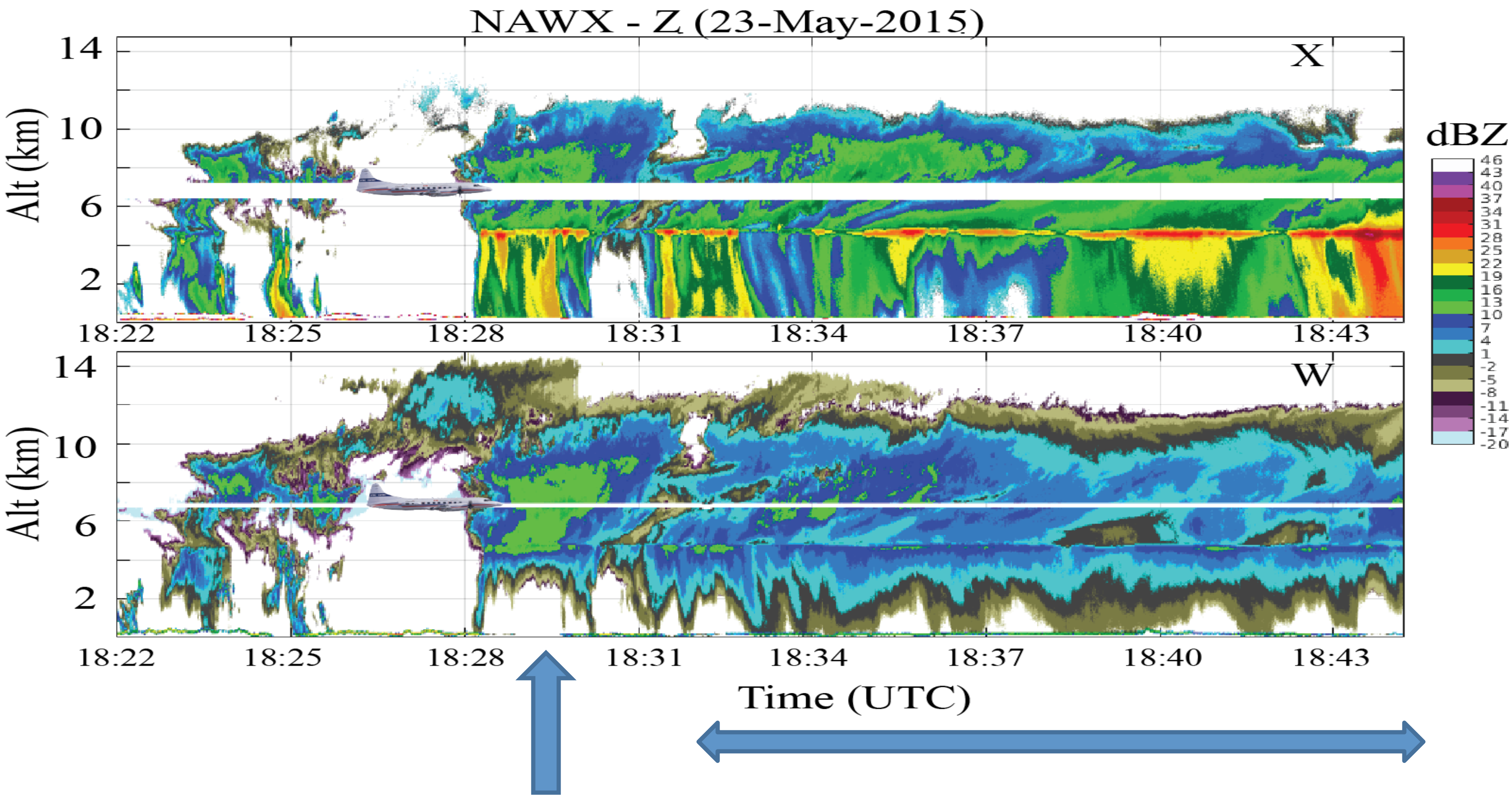

In rain – W-band heavy attenuation
At flight level – good agreement b/n X and W

Flight level – Mie effect – large crystals

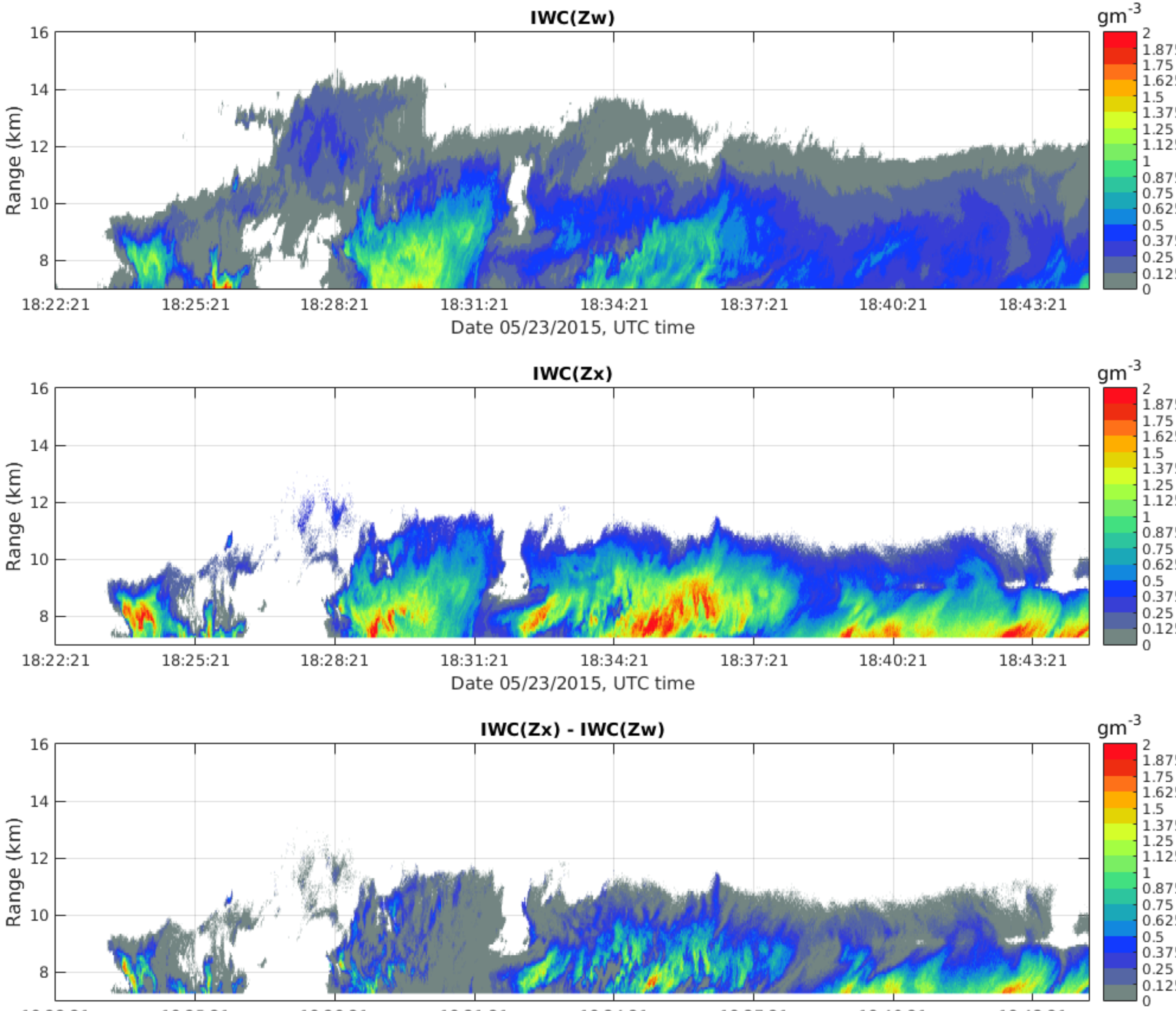
IWC(Zw)
gm-3
Range (km)
Date 05/23/2015, UTC time
18:22:21
18:25:21
18:28:21
18:31:21
18:34:21
18:37:21
18:40:21
18:43:21
IWC(Zx)
IWC(Zx) - IWC(Zw)

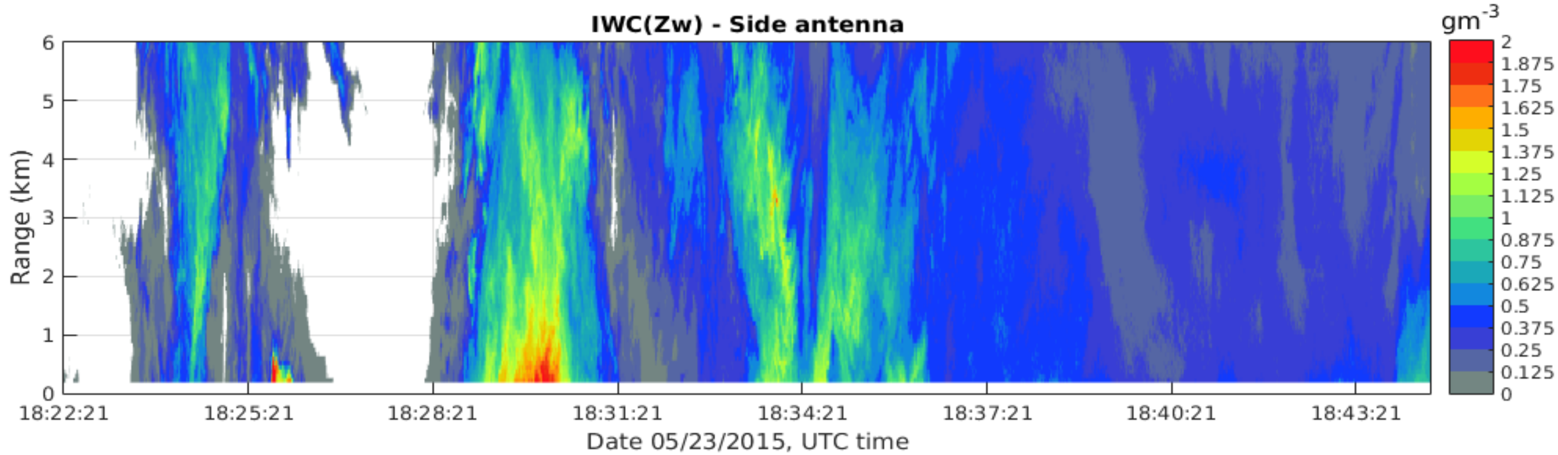
IWC(Zw) - Side antenna
Range (km)
Date 05/23/2015, UTC time
gm-3
18:22:21
18:25:21
18:28:21
18:31:21
18:34:21
18:37:21
18:40:21
18:43:21

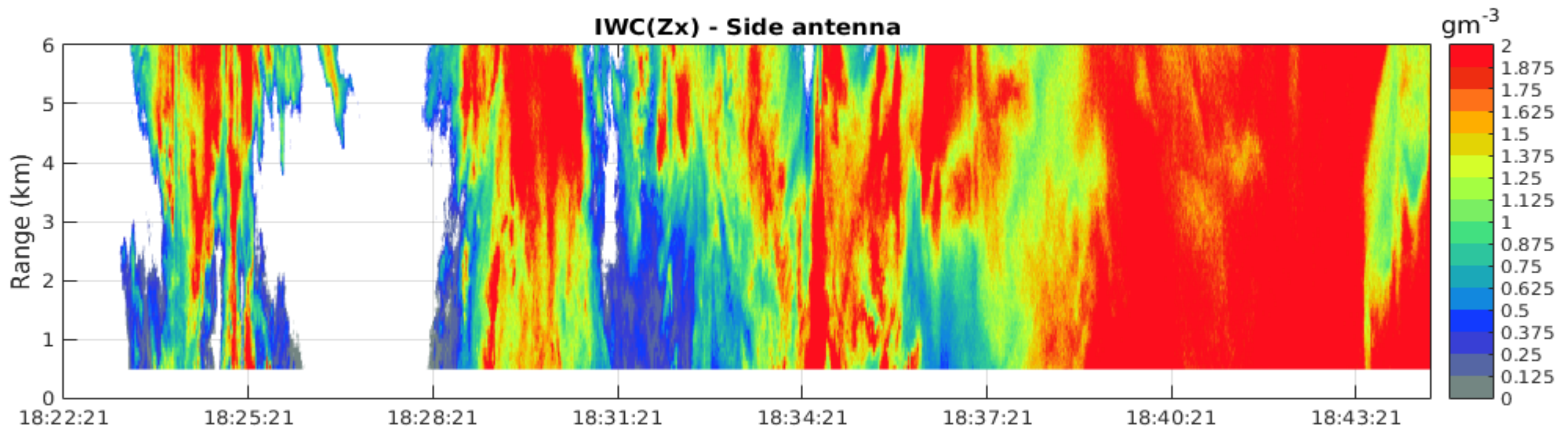
IWC(Zx) - Side antenna
Range (km)
gm-3
18:22:21
18:25:21
18:28:21
18:31:21
18:34:21
18:37:21
18:40:21
18:43:21

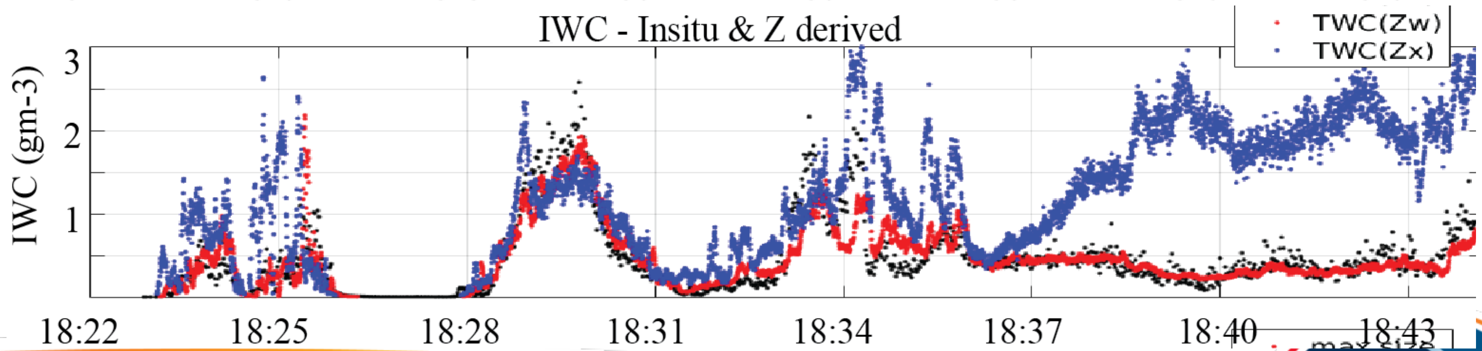
IWC - Insitu & Z derived
IWC (gm-3)
TWC(Zw)
TWC(Zx)
18:22
18:25
18:28
18:31
18:34
18:37
18:40
18:43

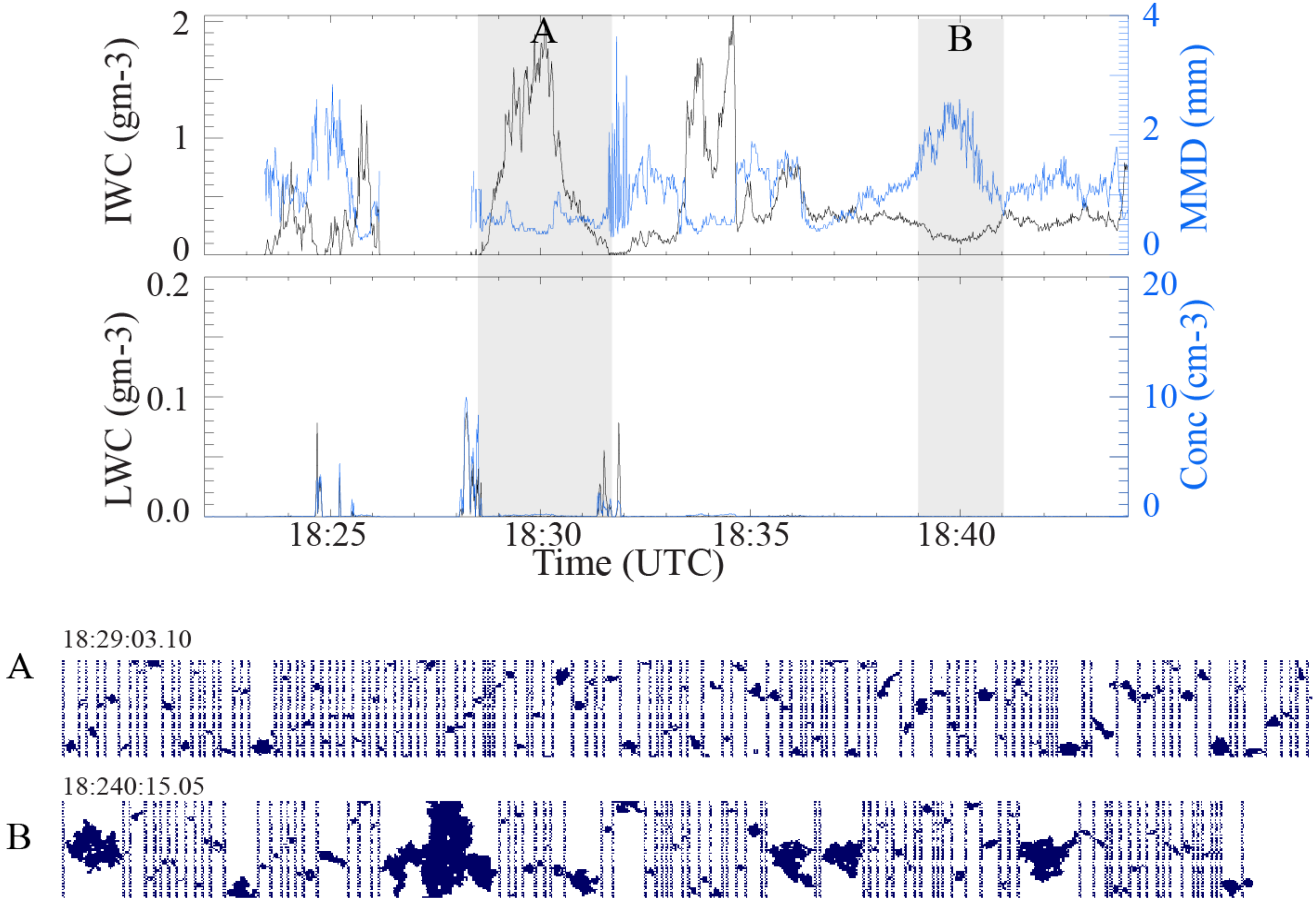

IWC (gm-3)
MMD (mm)
LWC (gm-3)
Conc (cm-3)
Time (UTC)
A
B
2
1
0
4
2
0
0.2
0.1
0.0
20
10
0
18:25
18:30
18:35
18:40
18:29:03.10
18:240:15.05

Polarimetric method for HIWC identification and estimation

Background

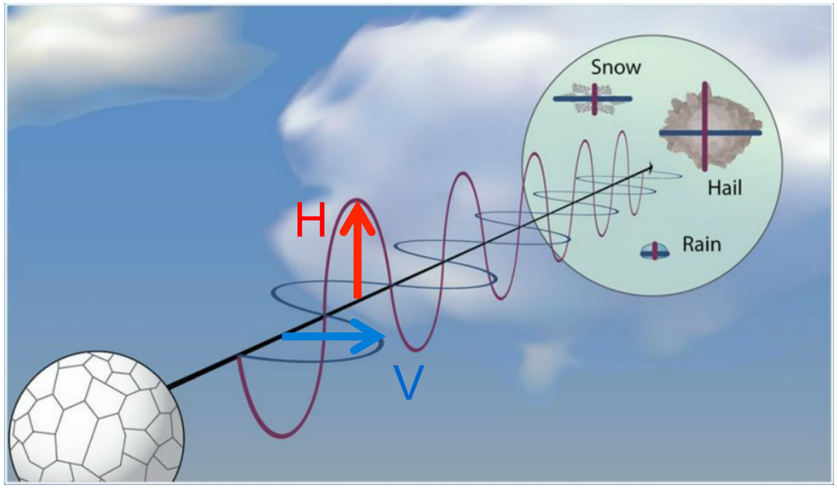

Courtesy: http://www.nws.noaa.gov/

$$Z_{h,v} = \lambda^4 / \pi^5 K^2 \int \sigma_{h,v} N(D)$$

$$K_{dp} = 180\lambda/\pi \int Re(f_h - f_v) N($$

$$\sigma_h - \sigma_v / Re(f_h - f_v) = 2\pi^2$$

Conventional estimation of specific differential phase K_{dp}

$$\Psi_{dp} = arg\{\langle H_i^* V_i \rangle\}$$

$$\Psi_{dp} = \Phi_{dp} + \delta_{dp}$$

$$K_{dp}(r) = 1/2\, d\Phi_{dp}(r)/dr$$

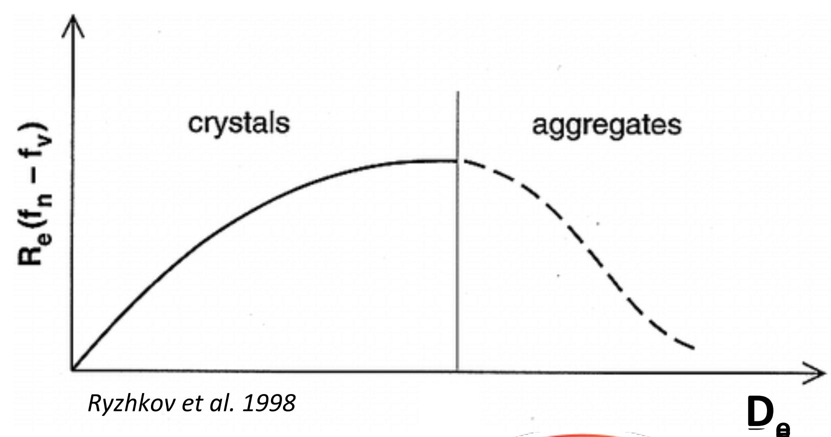

Ryzhkov et al. 1998

The NAWX system

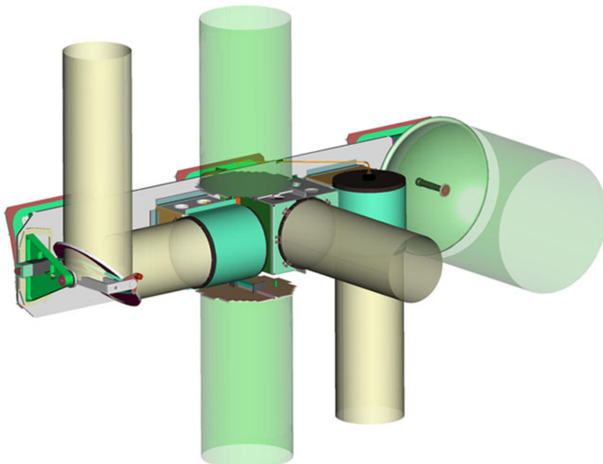

W band: pale yellow

	X-band	W-band
RF output frequency	9.41 GHz +/- 30 MHz	94.05 GHz
Peak transmit power	25 kW magnetron split between two ports	1.7 kW typical
Transmit polarization	H and V	H or V
Maximum Pulse Repetition Rate	5 kHz	15 kHz
Receivers	2	2
Receiver polarization	simultaneous H and V	co and cross-polarization
Processing	Pulse pair and FFT	Pulse pair, FFT, PDPP and raw (IQ)
Antennas	**Side: 1 x 26” dual-pol** Nadir/Zenith: 2 x 18” single-pol	**Side/Aft: 2 x 12” dual-pol** Nadir/Zenith: 1 x 12” single-pol

Method for estimation of K_{dp}

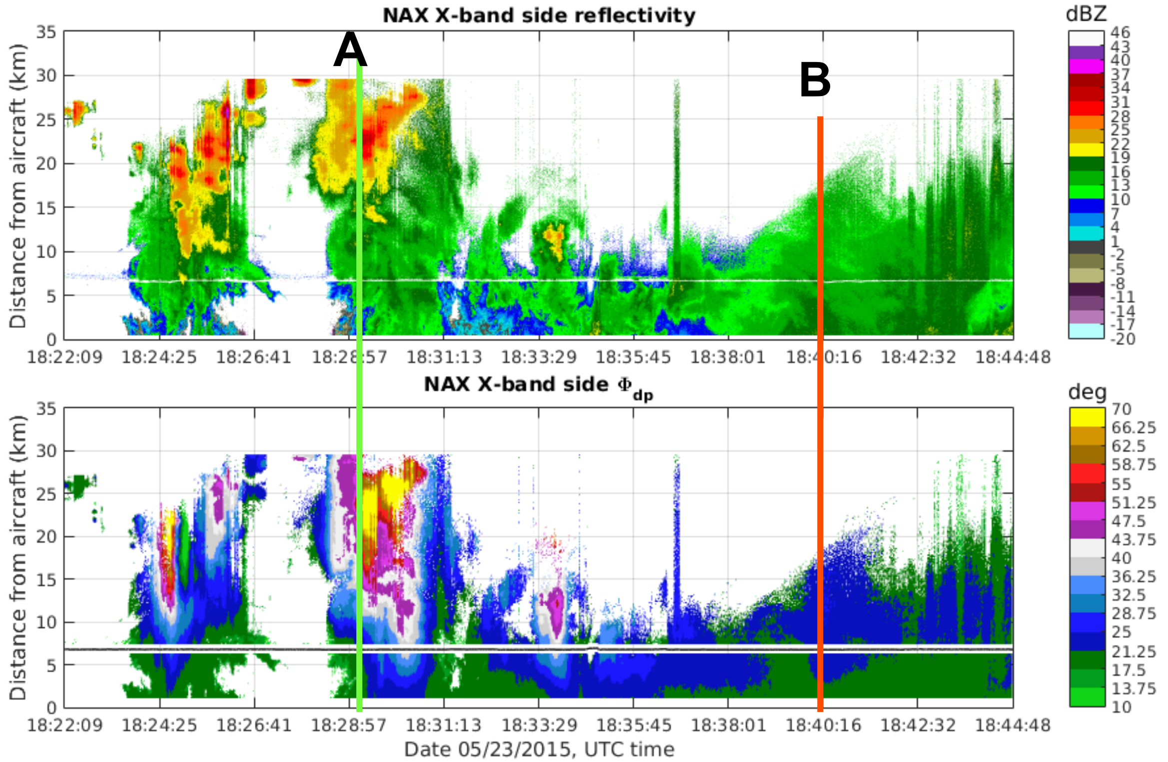

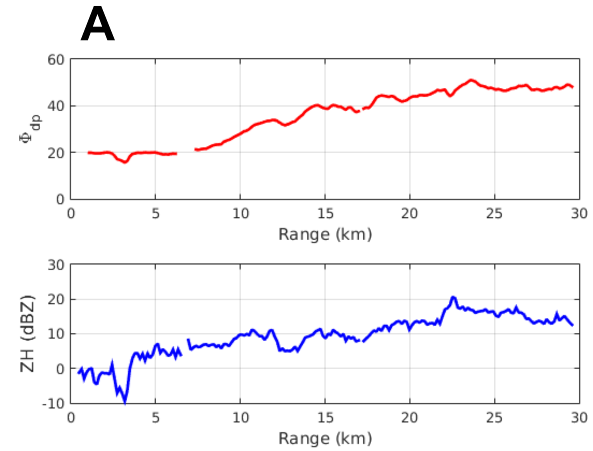

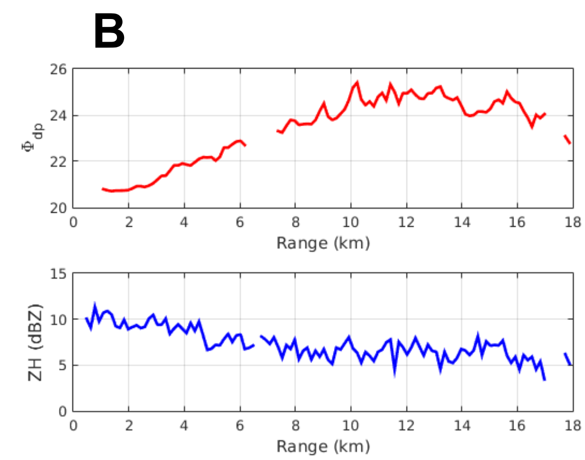

NRC K_{dp} estimator

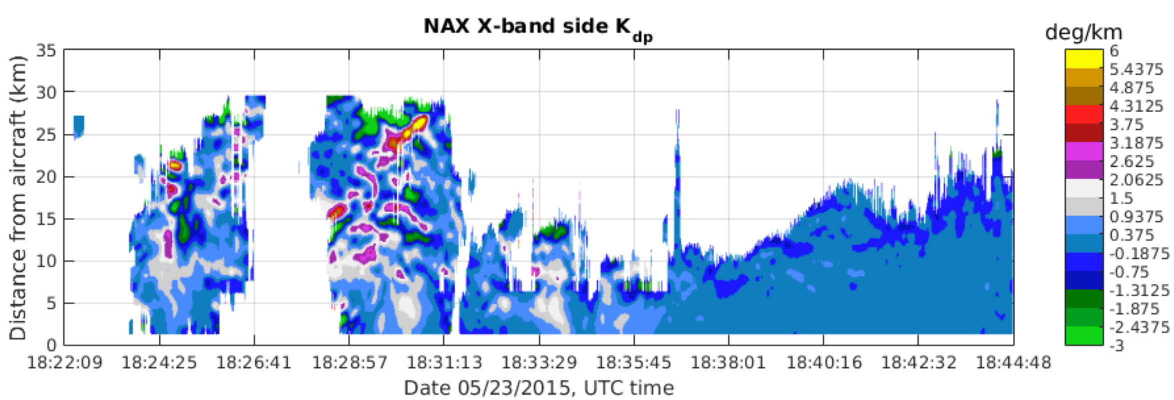

Case Study: May 23

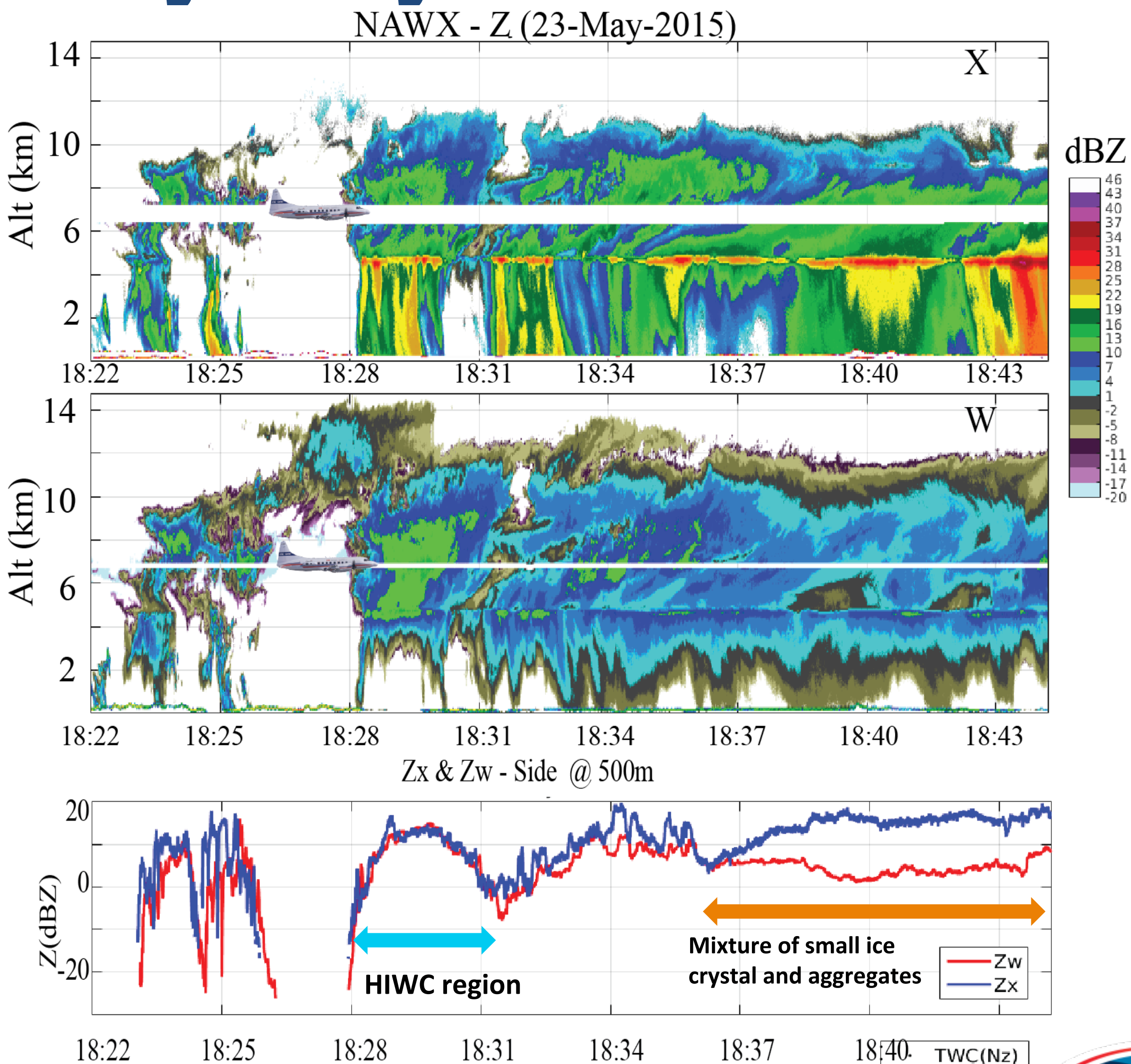

Case Study: May 23

IWC retrieval using Kdp(X)

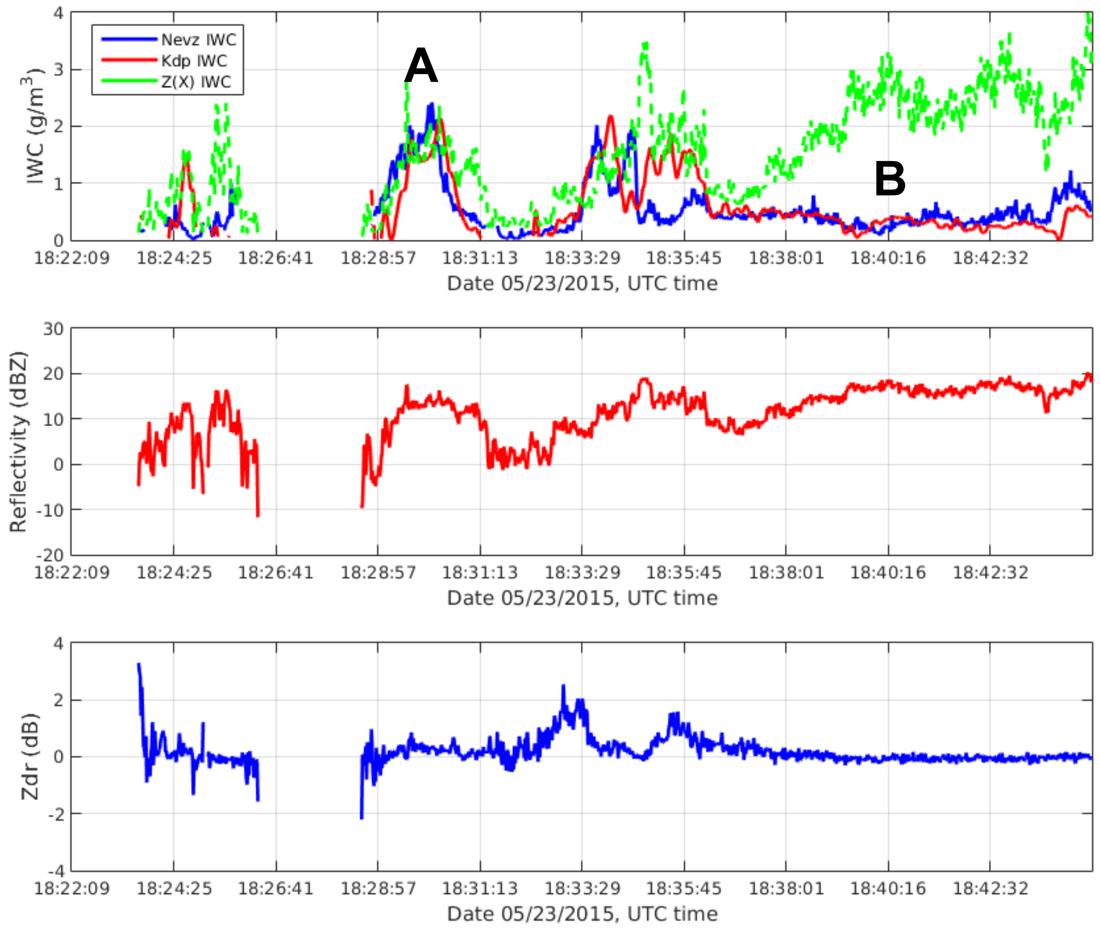

Case Study: May 23

Map Z(X) and est.

IWC retrieval using Kdp(X)

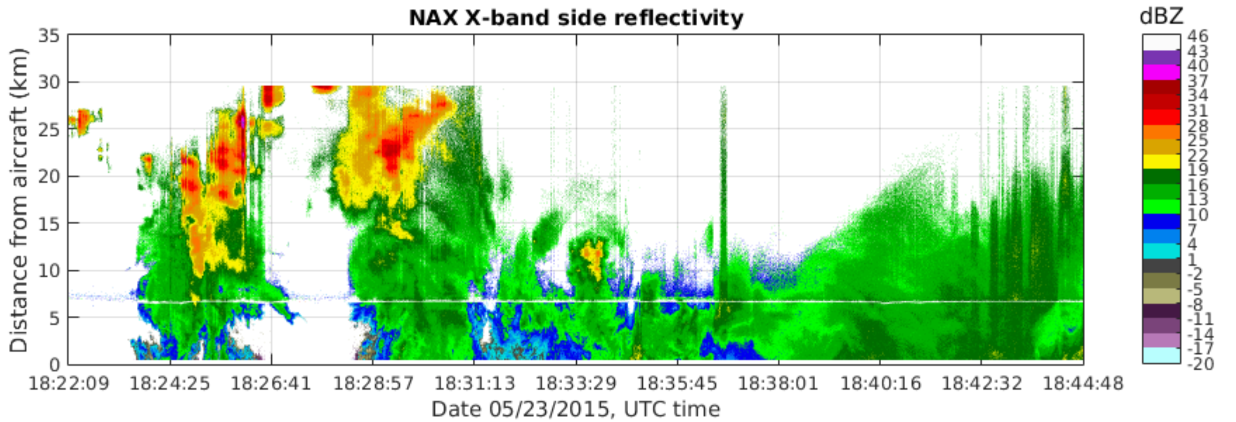

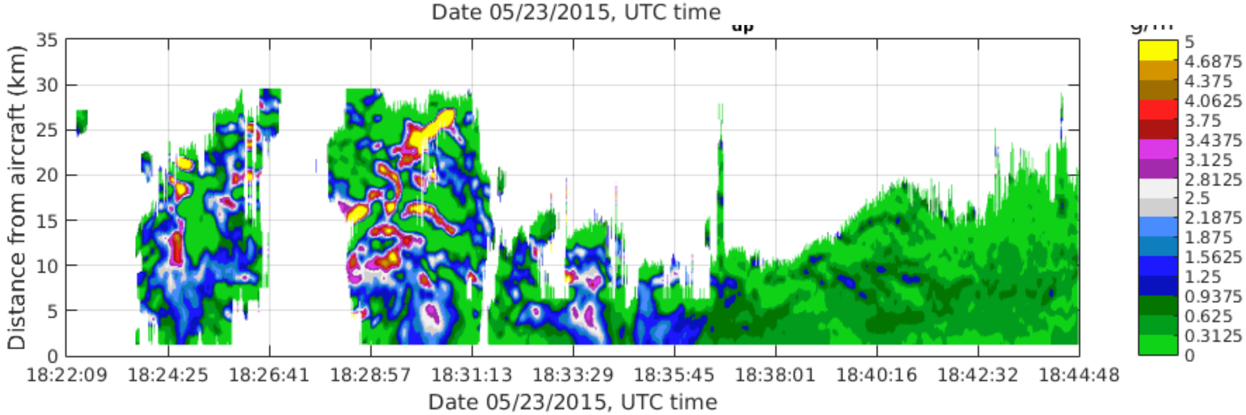

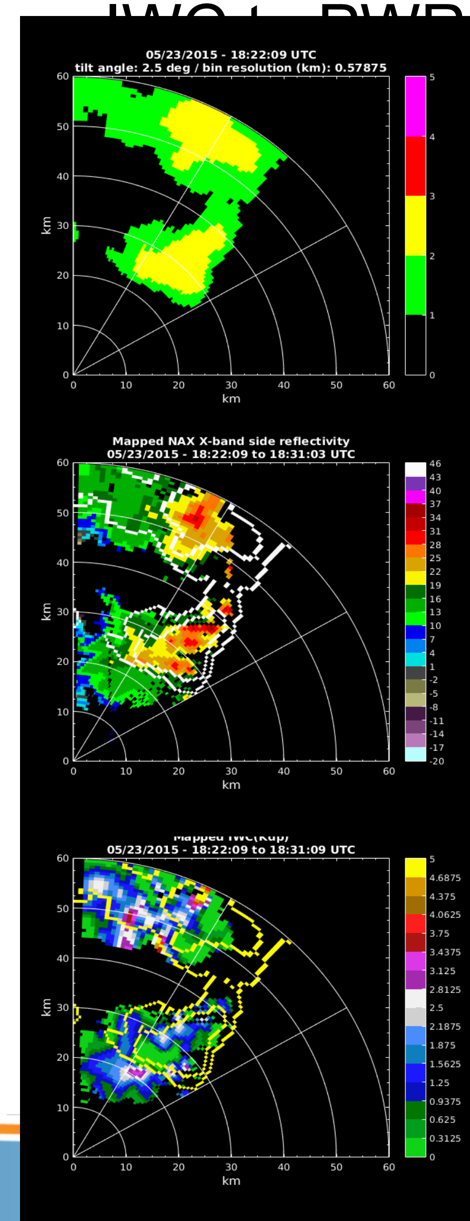

Future work

- IWC – Kdp, Zdr, T relationship (X-band)
- Above + polarimetric W-band
- Retrieval algorithm using polarimetric X-band, W-band and lidar/radiometer

NRC·CNRC

IWC - Lidar

Putting it all together…

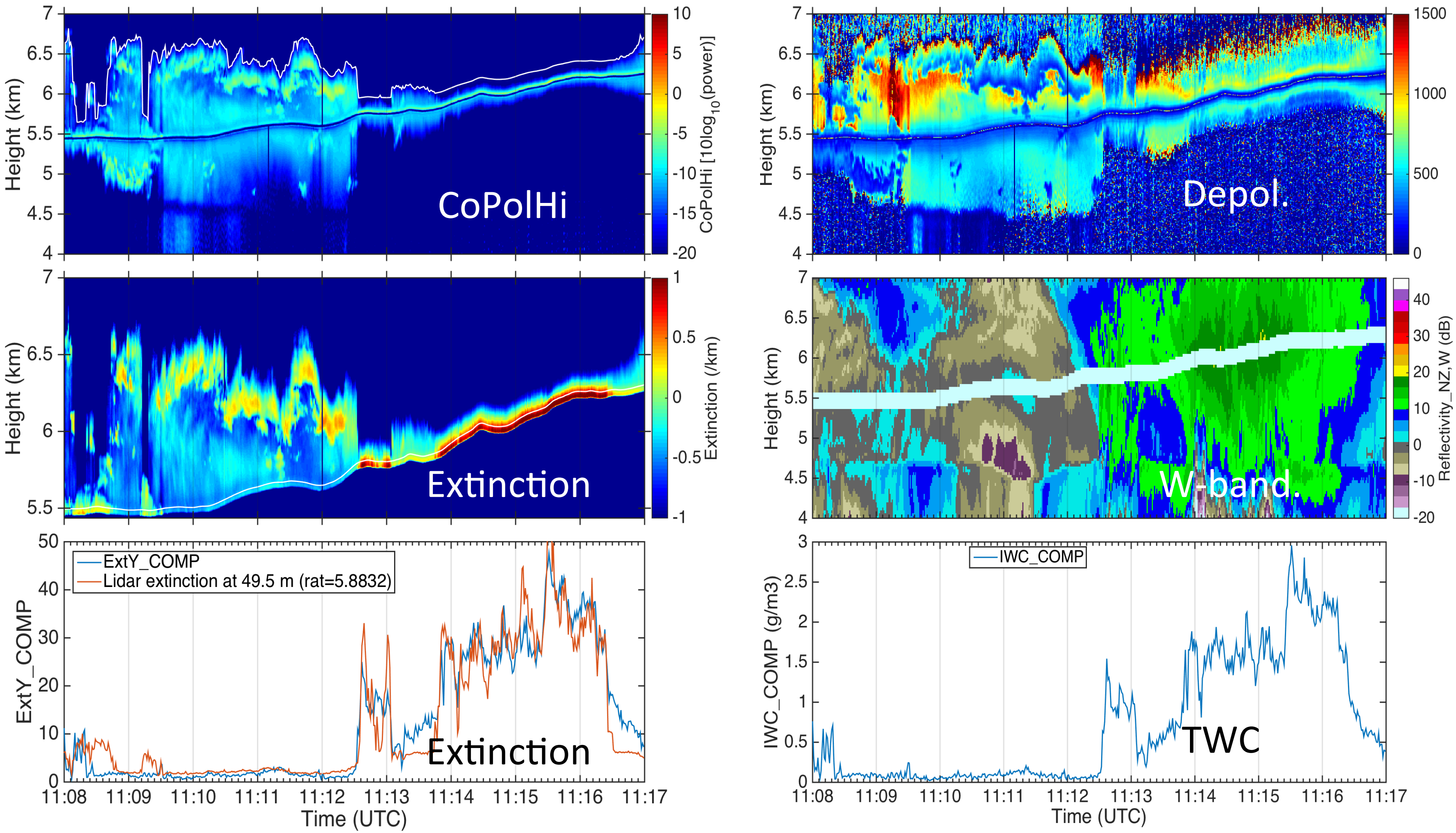

23-May;Increasing extinction

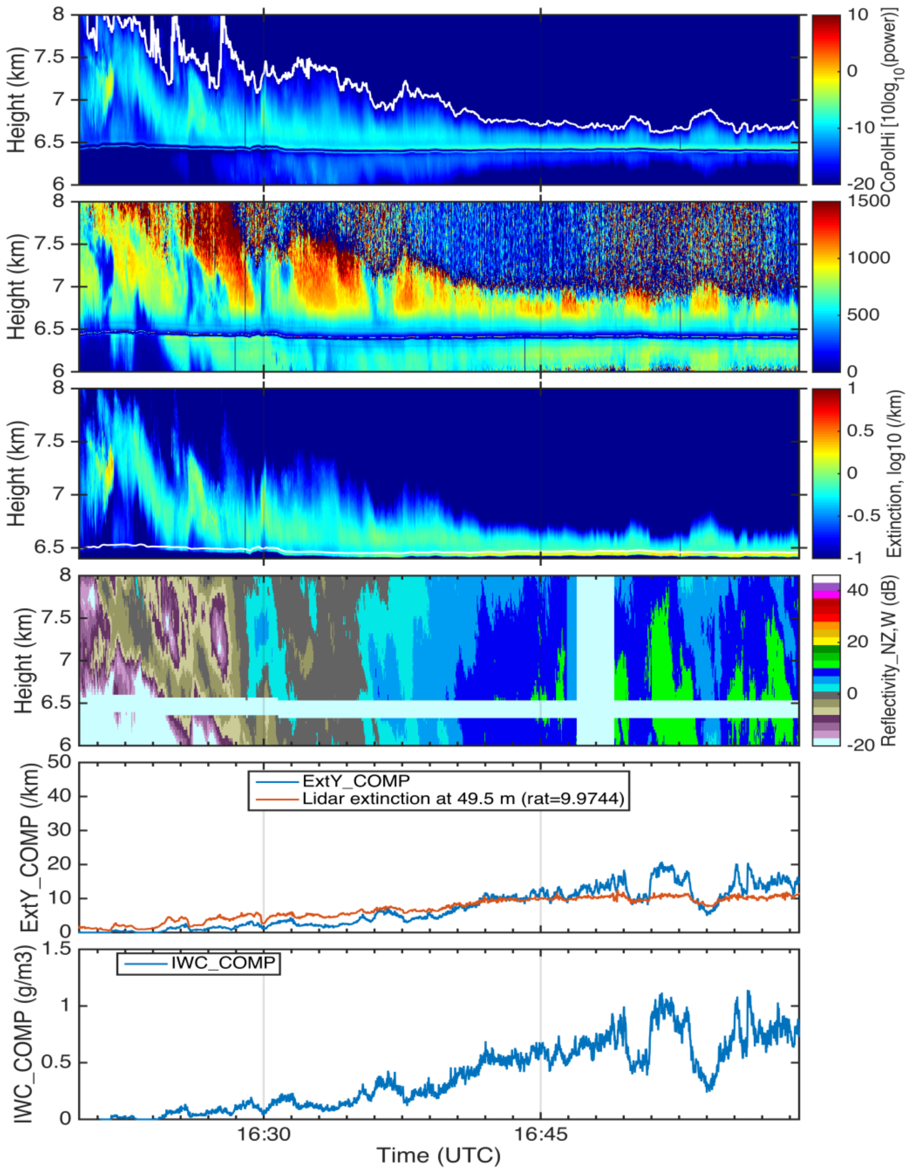

20-May;Decreasing extinction

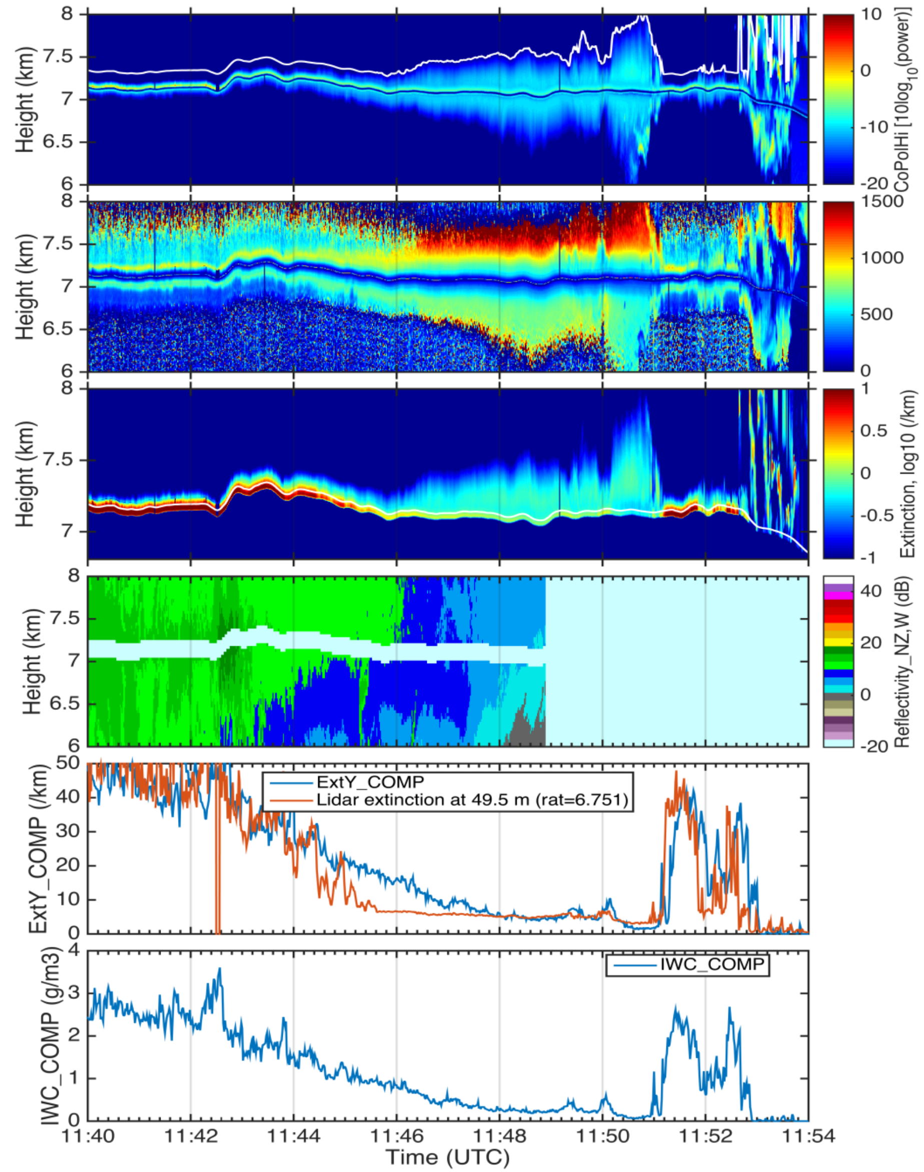

Fine-scale structure

May 15, 2015 | May 23, 2015

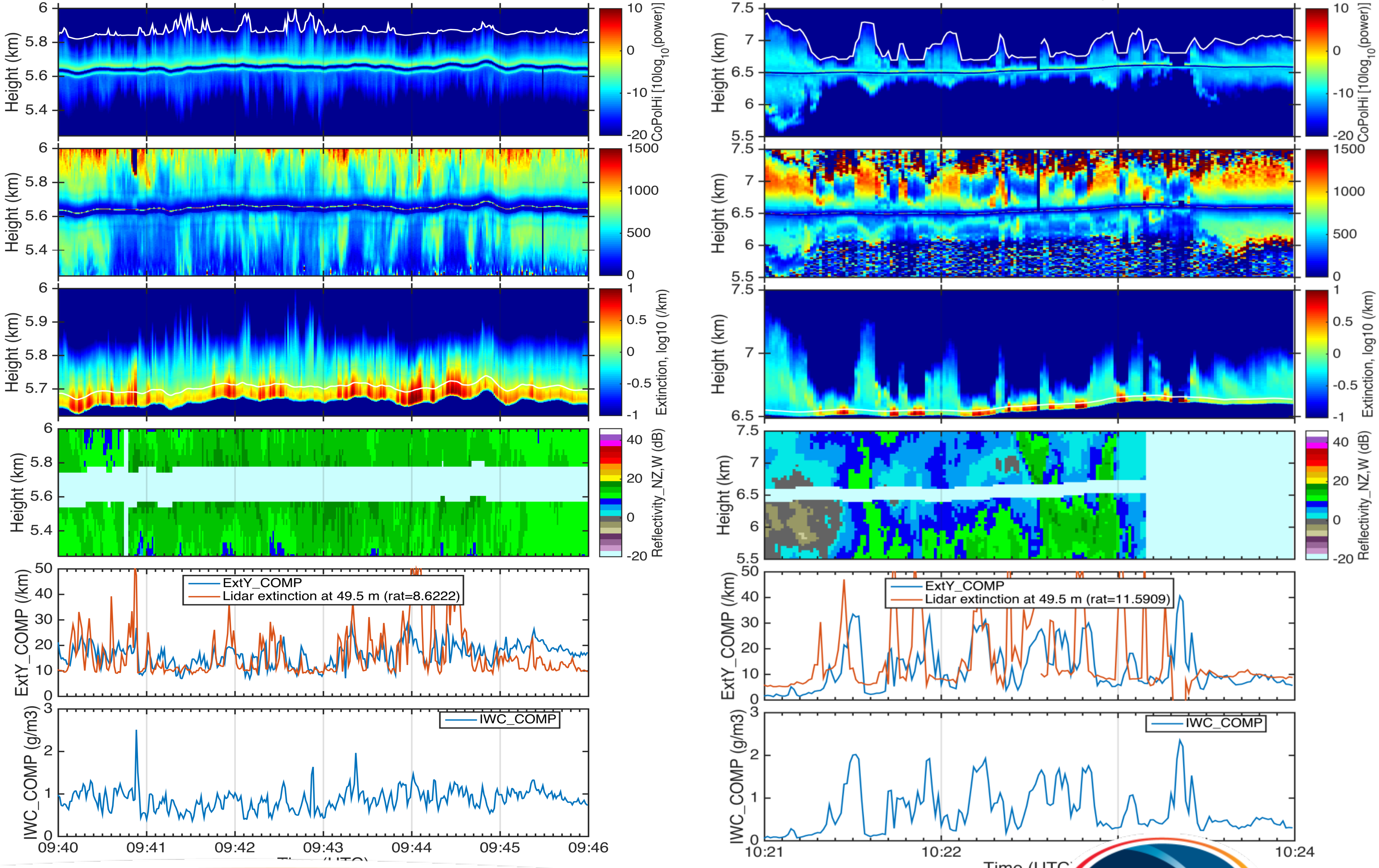

Future tasks

- Klett inversions in the nadir direction
- Klett sensitivity to the initial conditions: reference range, reference extinction/backscatter value, lidar ratio.
- Multiple-scattering correction
- Depolarization ratio (absolute values)
- Time synchronization
- Zenith and nadir return power coherency
- More test case analysis

Simulations of 183 Ghz GVR Microwave Brightness Temperatures for Ice Clouds Over Ocean Water

G-band (183 GHz) water Vapor Radiometer (GVR)

- Developed by ProSensing Inc. and first airborne installation on Convair in 2007 (Pazmany & Wolde, 2009)

- Measures brightness temperature at 183.31 ±1, ±3, ±7 and ± 14 GHz

- Neural Network Retrievals of PWV and LWP from GVR brightness temperature (Pazmany, 2009; Cadeddu et. al., 2009)

Example of GVR responses to the HIWC environemnt:17– 09:55:41 UTC

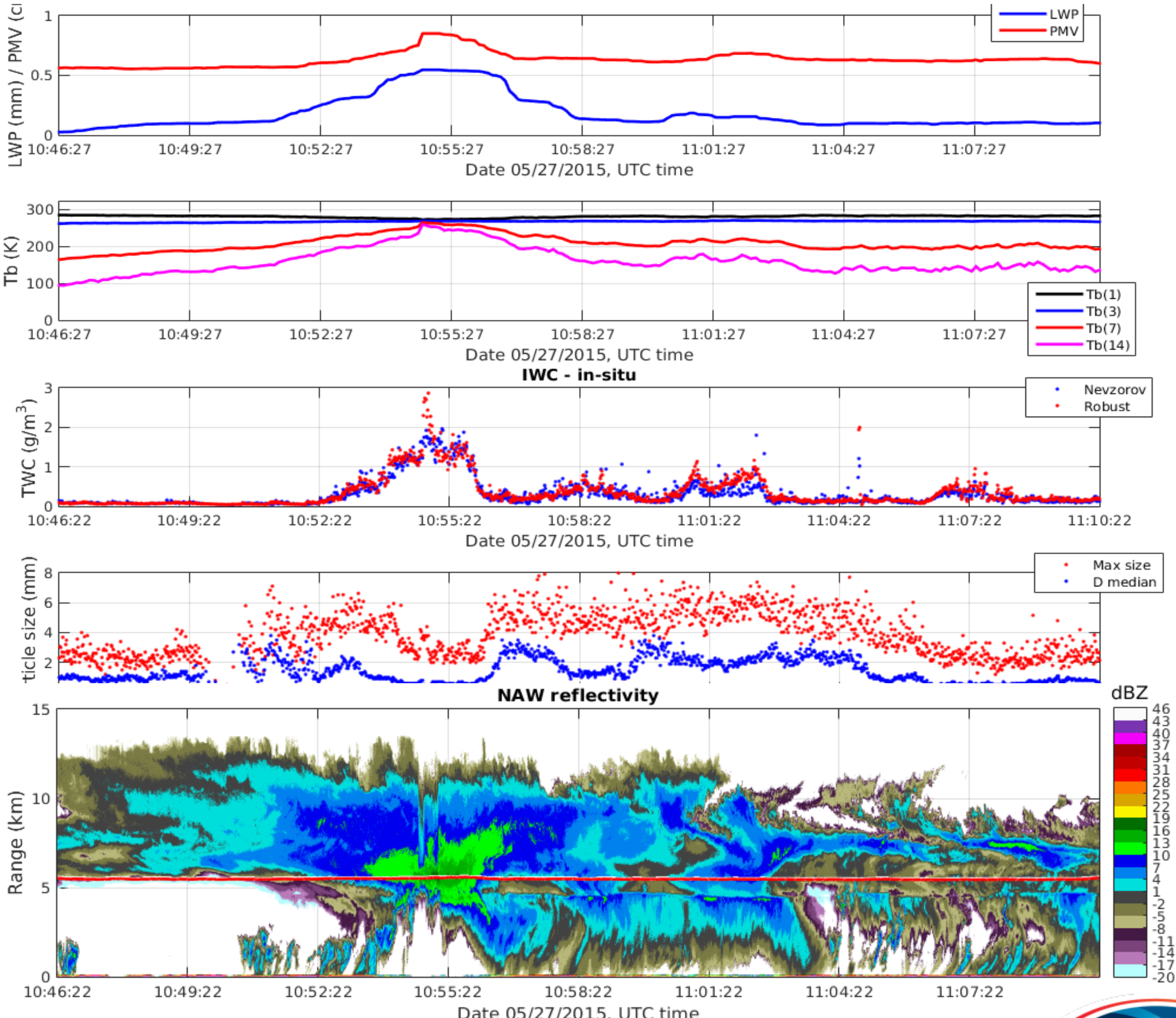

Objective

Scalar radiative transfer simulations of brightness temperatures were compared to those mmeasured by the GVR radiometer to ascertain:

- the sensitivity of the latter to thermodynamic/optical properties of the cloud and atmosphere as well as the surface albedo
- to determine the consistency of the measured radiometric data.

Microwave scattering properties of water and ice particles

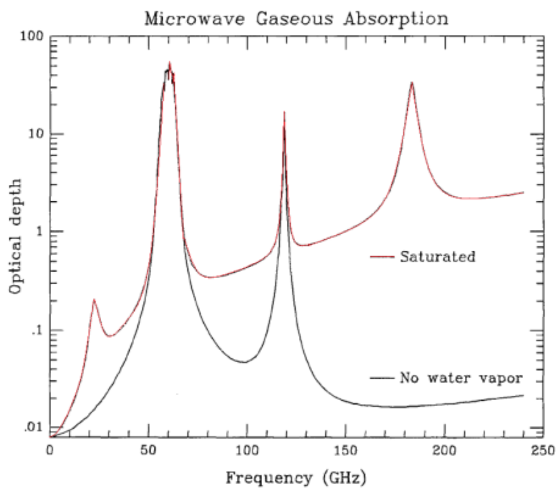

Optical depth as a function of frequency for the US standard atmosphere with no moisture and with 100% relative humidity. At the GVR frequencies, the relative humidity introduces significant absorption. Thus the accurate computation of the latter requires knowledge of the vertical distribution of water vapor.

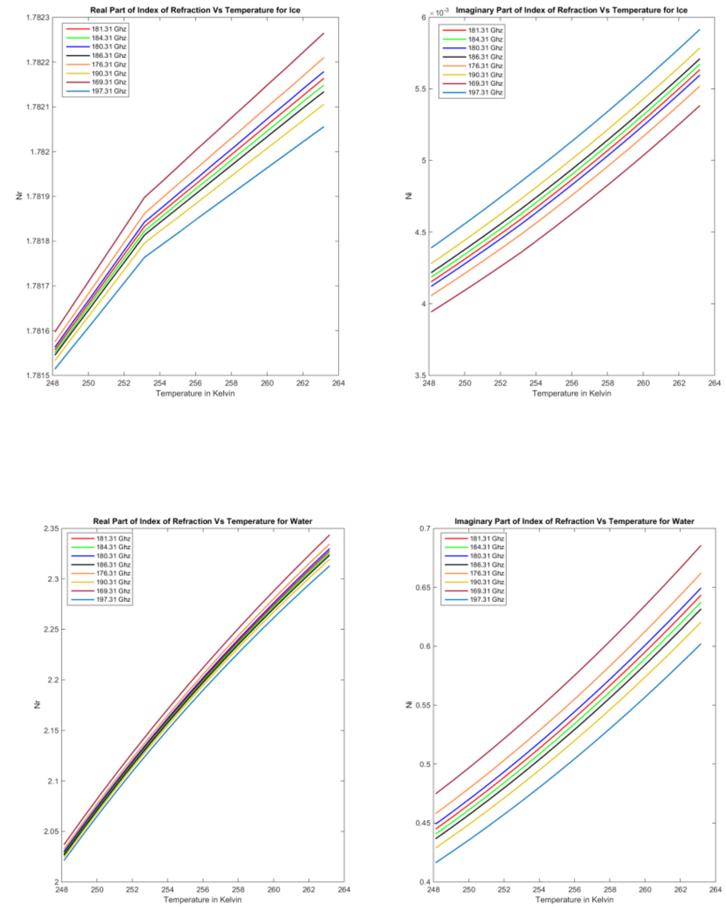

Variation of the real and imaginary components of the index of refraction of ice with frequency and temperature. The index of refraction is used to calculate the Mie scattering properties of the spherical ice particles.

Sensitivity Analysis

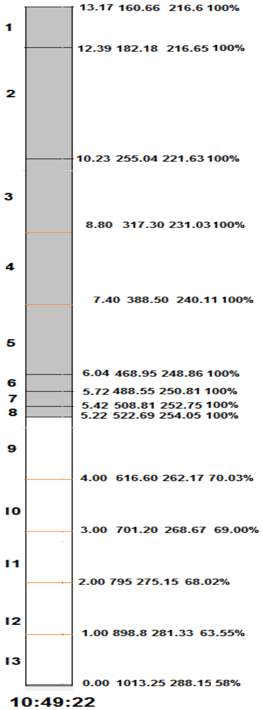

Model cloud, comprised of ice particles, with upper and lower boundaries deduced from radar range gates at time 10:49:22.

Sensitivity of brightness temperatures at the 8 GVR frequencies to biases in pressure, temperature, relative humidity, particle number concentration and surface albedo.

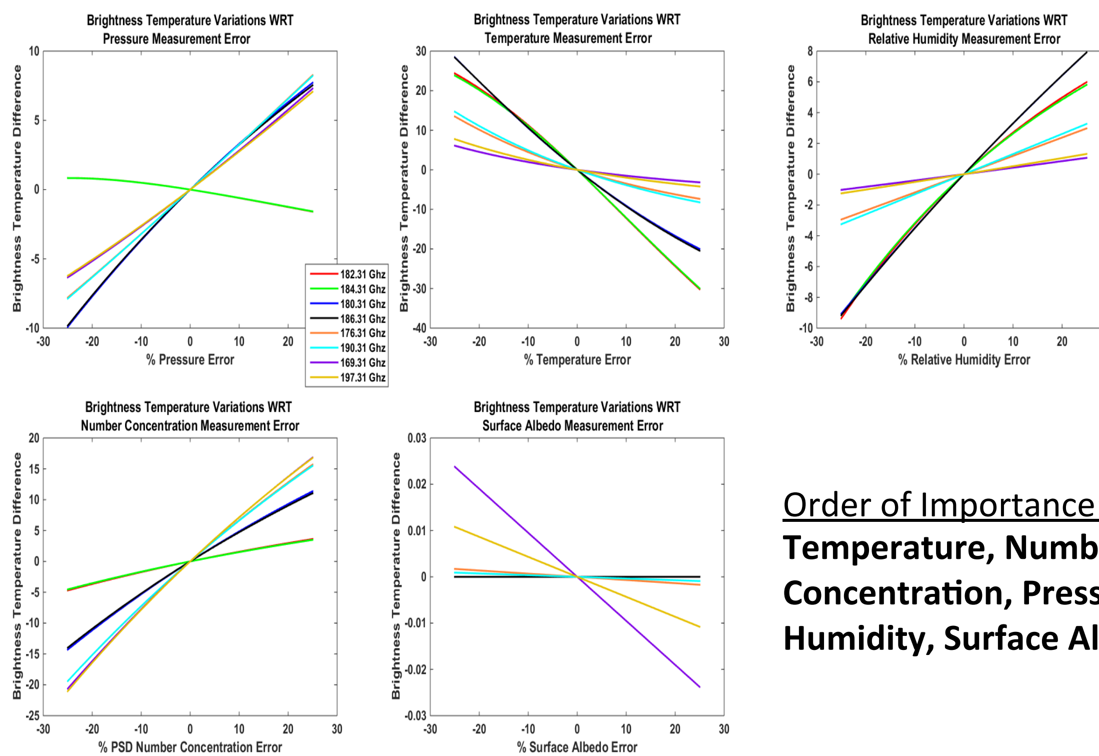

Order of Importance:

Temperature, Number Concentration, Pressure, Humidity, Surface Albedo

Effect of Column Optical Depth Averaging on Brightness Temperature Calculations

The purpose of this analysis was to compare radiances calculated without (vertical) spatial averaging of the optical properties to cases where such averaging was employed. The four cases analyzed in detail were selected manually at the times indicated by the red vertical lines in the figure. At these times, the cloud exhibits plane parallel characteristics and contains mainly ice particles. The layers altitude, pressure, temperature and relative humidity) are shown below. Results are illustrated In the next slide.

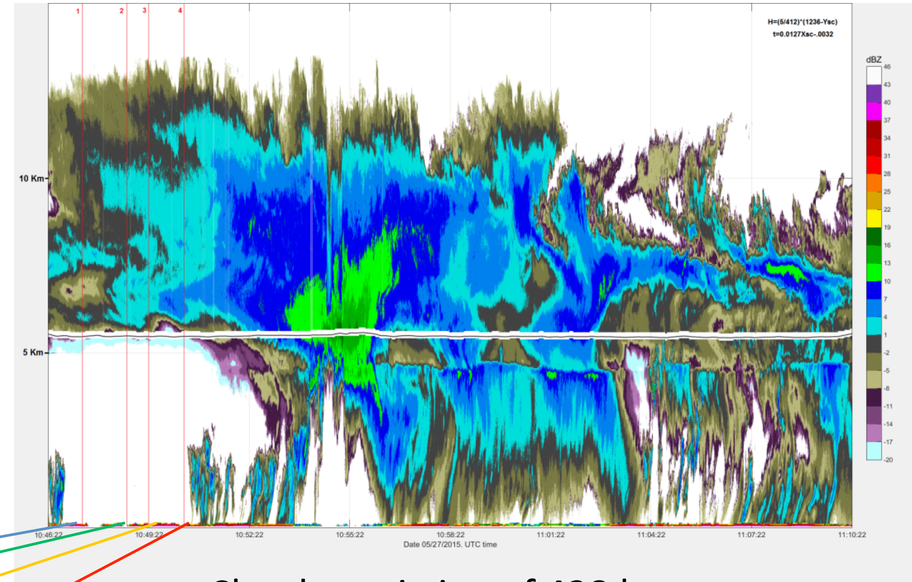

Cloud consisting of 438 layers.

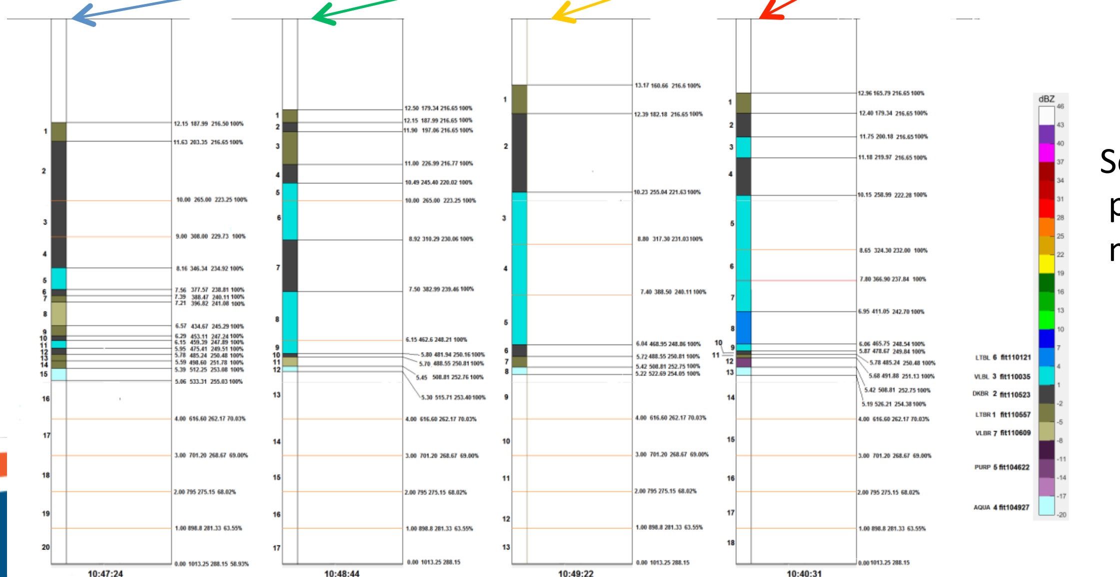

Selected vertical cloud distributions exhibiting plane parallel characteristics and containing mainly ice particles

Simulated Brightness Temperatures Along the Flight Path

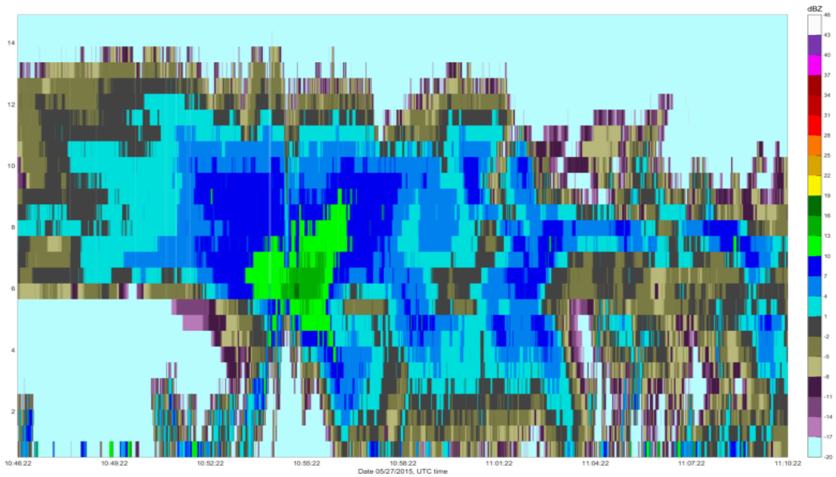

Averaged cloud, consisting of 29 layers.

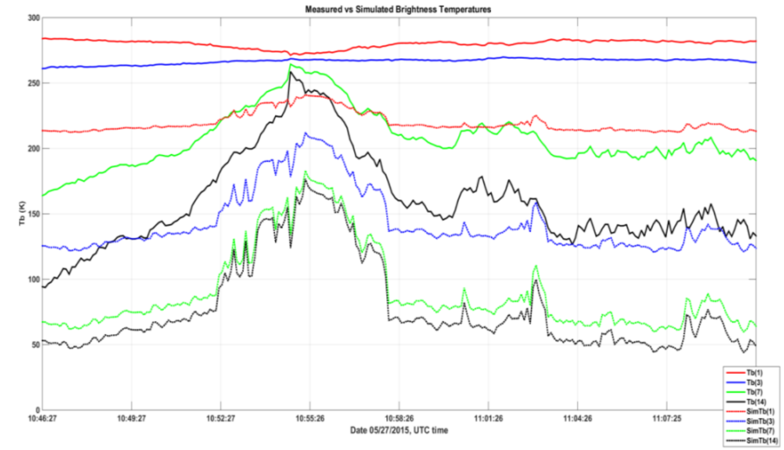

Brightness temperature measurements compared to simulations**.** Time interval is 6.0 seconds, or 239 measurements.

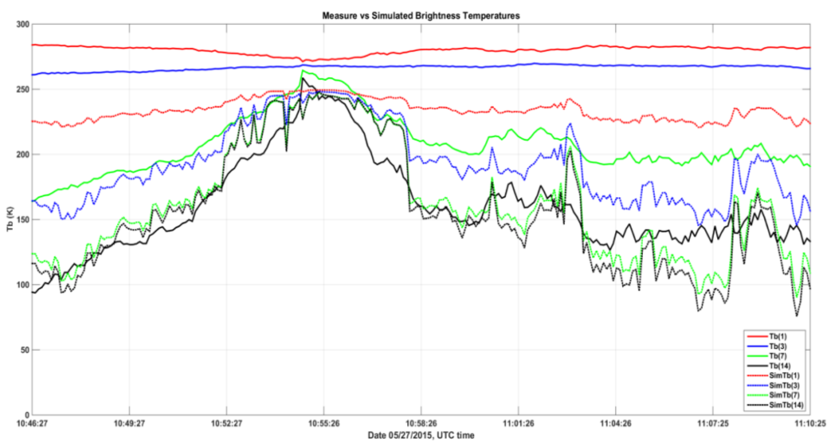

As above (right panel) but with the cloud optical depth multiplied everywhere by a factor of five.

Results of radiative transfer simulations are In broad qualitative agreement with observations, considering the absence of the thermodynamic structure of the atmosphere and the PSD within the cloud.